JOURNAL OF GUIDANCE, CONTROL, AND DYNAMICS
Vol. 28, No. 6, November–December 2005

Fuel-Optimal, Power-Limited Rendezvous with Variable Thruster Efficiency

Giovanni Mengali* and Alessandro A. Quarta†
University of Pisa, I-56122 Pisa, Italy

The problem of minimum-fuel, time-fixed, three-dimensional rendezvous for a solar electric propulsion spacecraft is discussed. The problem is solved via an indirect approach. The formulation takes into account both a variable bounded specific impulse and a variable thruster efficiency and permits us to manage solutions with coast arcs. The thruster efficiency is assumed to vary with the specific impulse through a polynomial approximation. The optimal specific impulse control law is found to depend on the instantaneous values of the primer vector modulus, the spacecraft mass, the mass costate, and the thruster model. Optimal interplanetary trajectories toward Mars are discussed. It is shown that the inclusion of a variable efficiency thruster model has important effects on fuel consumption. In particular, the classic constant efficiency thruster model overestimates the final spacecraft mass.

Nomenclature

$\hat{\boldsymbol{a}}$	=	unit thrust vector
c_k	=	polynomial approximation coefficients
$d_1, \ldots, d_5$	=	solar array power coefficients
f	=	function; see Eq. (17)
g_0	=	Earth's standard gravitational acceleration
H	=	Hamiltonian
H'	=	Hamiltonian depending on the control vector
I_{sp}	=	specific impulse
J	=	performance index
m	=	spacecraft mass
n	=	degree of polynomial approximation
P	=	maximum thruster input power
P_L	=	payload power
P_P^{max}	=	power processing unit maximum input power
P_{SA}	=	solar array power
$P_\odot$	=	solar array power at 1 astronomical unit from the sun
$\boldsymbol{r}$	=	position vector
t	=	time
$\mathcal{U}$	=	domain of feasible controls
$\boldsymbol{u}$	=	control vector
$\boldsymbol{v}$	=	velocity vector
η	=	thruster efficiency
η_P	=	duty cycle
λ_m	=	mass costate
$\boldsymbol{\lambda}_r$	=	vector adjoint to the position
$\boldsymbol{\lambda}_v$	=	primer vector
$\mu_\odot$	=	sun's gravitational parameter
τ	=	power throttle level

Subscripts

f	=	final
0	=	initial

Superscript

$\cdot$	=	time derivative

Received 27 July 2004; revision received 17 December 2004; accepted for publication 19 December 2004.

*Associate Professor, Department of Aerospace Engineering; g.mengali@ing.unipi.it.
†Research Assistant, Department of Aerospace Engineering; a.quarta@ing.unipi.it.

Introduction

AFTER the successful demonstration of the Deep Space 1, the first mission to be propelled by solar electric propulsion (SEP),[1] ion propulsion has become a very promising option available for future space missions. The striking advances in SEP technology have reduced greatly the costs and risks of using ion thruster as a primary propulsion system. Accordingly, in recent years, many studies have been performed to show the applicability and performance of SEP systems for space exploration.[2–7] The employment of SEP is especially interesting for those missions requiring large changes in orbital energy.[4,5] Moreover, SEP can help make many deep-space missions scientifically more attractive by allowing the use of smaller, less expensive launch vehicles and by reducing the trip times.[3] It has been also pointed out[6] that SEP missions to comets and asteroids may be accomplished without using complex gravity-assisted trajectories such as those needed for ballistic missions.

The problem of SEP-based mission design is also particularly interesting from a theoretical viewpoint, in that the thrust produced is very small and the engines are required to operate during most of the trajectory. This characteristic makes it a difficult task to find optimal trajectories and explains why a number of papers have been dedicated to this subject. However, most of the available literature concentrates on different techniques to find the optimal trajectory, rather than trying to use realistic thruster models.[8–11] It is well recognized that most of the benefits of SEP thrusters over conventional (or chemical) engines comes from the capability of the former to achieve a higher specific impulse. Clearly, the formulation of an optimal control problem for an SEP-based mission requires the inclusion of an adequate constraint for the thruster capability. From an analytical viewpoint, some interesting results have been achieved by Kechichian,[12] who discussed the minimum-fuel orbit transfer with variable, bounded specific impulse I_{sp}. Other contributions and extensions may be found by Carter and Pardis,[13] Vadali et al.,[14] Nah et al.,[15] and the references therein. All of these papers have a common denominator in that the thruster efficiency is assumed to be constant. However, this is a rather crude approximation because, as pointed out by Auweter-Kurtz and Kurtz,[16] the thruster efficiency strongly depends on the effective exhaust velocity and, hence, on the I_{sp}. On the other hand, the assumption of a constant thruster efficiency much simplifies the problem of deriving the optimal control law.

Only in a few cases, realistic SEP throttle performance has been incorporated into the trajectory optimization model. Williams and Coverstone-Carroll[4,5] and Sauer[7] used a polynomial approximation to describe thrust and mass flow rate as a function of the input power to the power processing unit (PPU). However, this approach greatly complicates the control law, which, indeed, is not explicitly found.

For these reasons, in this paper we revisit the problem of minimum-fuel orbit transfer by describing the thruster performance from a different viewpoint. When the experimental data of NASA SEP Technology Application Readiness (NSTAR) and NASA's Evolutionary Xenon Thruster (NEXT) thrusters are used, a best-fit polynomial is used to model the variation law of thruster efficiency with $I_{\rm sp}$. This allows us, for the first time, to derive an analytical expression for the control law with variable thruster efficiency and to investigate the mission performance as a function of the degree of polynomial approximation. The formulation permits the thruster to be switched off, thus, allowing coast phases in the optimal trajectory. An indirect method is employed to solve the minimum-fuel, fixed-time problem for the interplanetary phase of a sample Earth–Mars trajectory. For both thrusters, it is found that the assumption of a constant thruster efficiency introduces a significant error in the estimate of the total fuel consumption.

Mathematical Model

The equations of motion for a SEP spacecraft with mass m in a heliocentric inertial frame are

$$\dot{\boldsymbol{r}} = \boldsymbol{v} \tag{1}$$

$$\dot{\boldsymbol{v}} = -\frac{\mu_\odot}{r^3}\boldsymbol{r} + \frac{2\eta\tau P}{m g_0 I_{\rm sp}}\hat{\boldsymbol{a}} \tag{2}$$

$$\dot{m} = -\frac{2\eta\tau P}{g_0^2 I_{\rm sp}^2} \tag{3}$$

where $r \triangleq \|\boldsymbol{r}\|$ is the spacecraft distance from the sun. The vehicle is powered by a SEP system with variable specific impulse $I_{\rm sp}$, variable thruster efficiency η, maximum thruster input power P, and power throttle level $\tau \in [0, 1]$. Note that Eqs. (1–3) may be written in compact form form as

$$\dot{\boldsymbol{x}} = \boldsymbol{h}(\boldsymbol{x}, \boldsymbol{u}) \tag{4}$$

where $\boldsymbol{x} \triangleq [\boldsymbol{r}^T, \boldsymbol{v}^T, m]^T$ is the state vector and $\boldsymbol{u} \triangleq [\tau, I_{\rm sp}, \hat{\boldsymbol{a}}^T]^T$ is the control vector. The limits on the specific impulse are enforced through an inequality constraint, namely,

$$I_{\rm sp_{min}} \le I_{\rm sp} \le I_{\rm sp_{max}} \tag{5}$$

The behavior of the SEP system is modeled through three main elements[17]: 1) the solar array, 2) the PPU, and 3) the thrusters. The power available to the PPU equals the solar array power $P_{\rm SA}$ less the power allocated to operate the spacecraft systems P_L. The latter is assumed to be constant during the whole mission.[5] Not all of the power available to the PPU is supplied to the thrusters, and an efficiency $\eta_P < 1$ of the PPU (referred to as duty cycle) is taken into account. Accordingly, one has

$$P = \begin{cases} \eta_P\, P_P^{\max}, & \text{if} \quad P_{\rm SA} - P_L \ge P_P^{\max} \\ \eta_P\,(P_{\rm SA} - P_L), & \text{if} \quad P_{\rm SA} - P_L < P_P^{\max} \end{cases} \tag{6}$$

where $P_P^{\max}$ is the maximum input power to the PPU. The solar array power depends on the distance r through the following relationship[17]:

$$P_{\rm SA} = \frac{P_\odot}{r^2}\left(\frac{d_1 + d_2 r^{-1} + d_3 r^{-2}}{1 + d_4 r + d_5 r^2}\right) \tag{7}$$

where the term in brackets represents the relative array efficiency as a function of the empirical coefficients $d_1, \ldots, d_5$.

The thruster efficiency η is assumed to vary with the specific impulse according to the following polynomial approximation of degree n:

$$\eta = \sum_{k=0}^{n} c_k (I_{\rm sp})^k \tag{8}$$

where the coefficients c_k are chosen to fit the thruster experimental data.

Trajectory Optimization

The problem addressed here is to find the optimal control law $\boldsymbol{u}(t)$ (where $t \in [t_0, t_f]$) that minimizes the propellant mass necessary to transfer the spacecraft from an initial $(\boldsymbol{r}_0, \boldsymbol{v}_0)$ to a final $(\boldsymbol{r}_f, \boldsymbol{v}_f)$ prescribed state. Equivalently, the performance index

$$J = m_f \tag{9}$$

should be maximized, where m_f is the spacecraft mass at the fixed final time t_f. From Eqs. (1–3), the Hamiltonian associated with the problem is

$$H = \boldsymbol{\lambda}_r \cdot \boldsymbol{v} - \frac{\mu_\odot}{r^3}(\boldsymbol{\lambda}_v \cdot \boldsymbol{r}) + \frac{2\eta\tau P}{m g_0 I_{\rm sp}}(\boldsymbol{\lambda}_v \cdot \hat{\boldsymbol{a}}) - \frac{2\eta\tau P \lambda_m}{g_0^2 I_{\rm sp}^2} \tag{10}$$

where $\boldsymbol{\lambda}_r$ and $\boldsymbol{\lambda}_v$ are the vectors adjoint to the position and the velocity, respectively, and λ_m is the mass costate. The corresponding Euler–Lagrange equations are

$$\dot{\boldsymbol{\lambda}}_r = -\frac{\partial H}{\partial \boldsymbol{r}} = \frac{\mu_\odot}{r^3}\boldsymbol{\lambda}_v - \frac{3\mu_\odot(\boldsymbol{\lambda}_v \cdot \boldsymbol{r})}{r^5}\boldsymbol{r} - \frac{2\eta\tau}{m g_0 I_{\rm sp}}(\boldsymbol{\lambda}_v \cdot \hat{\boldsymbol{a}})\frac{\partial P}{\partial \boldsymbol{r}} + \frac{2\eta\tau\lambda_m}{g_0^2 I_{\rm sp}^2}\frac{\partial P}{\partial \boldsymbol{r}} \tag{11}$$

$$\dot{\boldsymbol{\lambda}}_v = -\frac{\partial H}{\partial \boldsymbol{v}} = -\boldsymbol{\lambda}_r \tag{12}$$

$$\dot{\lambda}_m = -\frac{\partial H}{\partial m} = \frac{2\eta\tau P}{m^2 g_0 I_{\rm sp}}(\boldsymbol{\lambda}_v \cdot \hat{\boldsymbol{a}}) \tag{13}$$

Without loss of generality, it is assumed that $\lambda_m(t_0) > 0$. Note that the gradient of P with respect to $\boldsymbol{r}$, which is required in Eq. (11), is obtained combining Eqs. (6) and (7). The result is

$$\frac{\partial P}{\partial \boldsymbol{r}} = \begin{cases} 0, & \text{if} \quad P_{\rm SA} - P_L \ge P_P^{\max} \\ -\boldsymbol{r} P_\odot \eta_P N(r)/D(r), & \text{if} \quad P_{\rm SA} - P_L < P_P^{\max} \end{cases} \tag{14}$$

where

$$N(r) \triangleq 4d_1d_5r^2 + (5d_2d_5 + 3d_1d_4)r + 6d_3d_5 + 4d_2d_4 + 2d_1 + (5d_3d_4 + 3d_2)/r + 4d_3/r^2$$

$$D(r) \triangleq r^4\left(1 + d_4 r + d_5 r^2\right)^2 \tag{15}$$

From the Pontryagin's maximum principle, the optimal control law $\boldsymbol{u}(t)$, to be selected in the domain of feasible controls $\mathcal{U}$, is such that, at any time, the Hamiltonian is an absolute maximum. This amounts to maximizing the function H', which coincides with that portion of the Hamiltonian H that explicitly depends on the control vector, that is,

$$\boldsymbol{u} = \arg\max_{u \in \mathcal{U}} H \equiv \arg\max_{u \in \mathcal{U}} H' \quad \text{with} \quad H' \triangleq \frac{2\eta\lambda_v\tau P}{m g_0 I_{\rm sp}}\hat{\boldsymbol{a}} \cdot \left(\hat{\boldsymbol{\lambda}}_v - \frac{f}{I_{\rm sp}}\hat{\boldsymbol{a}}\right) \tag{16}$$

where $\hat{\boldsymbol{\lambda}}_v \triangleq \boldsymbol{\lambda}_v/\lambda_v$ is the direction of the primer vector,[18] $\lambda_v = \|\boldsymbol{\lambda}_v\|$, and

$$f \triangleq m\lambda_m/(g_0\lambda_v) \tag{17}$$

is a time function whose instantaneous value univocally defines the optimal $I_{\rm sp}$ control law, as discussed later.

To maximize H', consider first the thrust vector. As long as $\boldsymbol{\lambda}_v \neq 0$, Eq. (16) implies that $\hat{\boldsymbol{a}}$ is parallel to the primer vector $\boldsymbol{\lambda}_v$ (Refs. 12 and 13), that is,

$$\hat{\boldsymbol{a}} = \hat{\boldsymbol{\lambda}}_v \tag{18}$$

Table 1 Polynomial coefficients of η for NSTAR thruster[a] and NEXT thruster[b]

n	c_0	$c_1 \times 10^{-4}$, s^{-1}	$c_2 \times 10^{-7}$, s^{-2}
		NSTAR	
0	0.62		
1	0.0787	1.7022	
2	0.7622	−3.9677	1.1070
		NEXT	
0	0.68		
1	0.2916	0.9624	
2	0.1424	1.9231	−0.1499

[a]Derived from Ref. 20. [b]Derived from Ref. 21.

whereas $\tau = 0$ whenever $\lambda_v = 0$. With the aid of Eq. (18), Eq. (13) shows that $\dot{\lambda}_m \geq 0\ \forall t \geq t_0$. Accordingly, Eq. (17) implies that $f > 0$ because, by assumption, $\lambda_m(t_0) > 0$. Also note that Eq. (16) may be rewritten as

$$H' = \frac{2\eta\lambda_v \tau P}{m g_0 I_{sp}}\left(1 - \frac{f}{I_{sp}}\right) \tag{19}$$

and H' is now a function only of the two independent controls τ and I_{sp}. The optimal control law for τ is found observing that H' depends linearly on τ. As a result, a bang–bang control is optimal.[19] Because $H' > 0$ if and only if $I_{sp} > f$, one obtains

$$\tau = \begin{cases} 1, & \text{if} \quad f < I_{sp_{max}} \\ 0, & \text{if} \quad f \geq I_{sp_{max}} \end{cases} \tag{20}$$

Equation (20) implies that whenever $f \geq I_{sp_{max}}$ the optimal value of the specific impulse should not be calculated because, in that case, a coast phase takes place. Therefore, assume $f < I_{sp_{max}}$. Our aim is to find the optimal value of I_{sp}. When it is recalled that the thruster efficiency is given by Eq. (8) and the necessary condition $\partial H'/\partial I_{sp} = 0$ is invoked, Eq. (19) yields

$$f = \frac{\sum_{k=0}^{n}(1-k)c_k(I_{sp})^{(k+1)}}{\sum_{k=0}^{n}(2-k)c_k(I_{sp})^k} \tag{21}$$

which is valid, as long as $\lambda_v \neq 0$, for any integer n. In practice, sufficiently accurate approximations for η are obtained setting $n = 2$.

Equation (21) states that the optimal impulse is closely connected to the instantaneous value of f, which depends on the primer vector modulus, the spacecraft mass, and the mass costate, according to Eq. (17).

The optimal control laws for $n = 0$, 1 and 2 are now investigated, where the coefficients c_k are those of the NSTAR[20] and NEXT[21] thrusters (Table 1).

Quadratic Approximation of η

When $n = 2$ is substituted into Eq. (8), a reasonable approximation of η vs I_{sp} is obtained (Figs. 1 and 2).

The optimal control law for the specific impulse is better discussed with the aid of a geometrical approach. Let $\mathcal{S}$ be the region of the plane (f, I_{sp}) that satisfies the following four conditions: 1) $H' \geq 0$, 2) $\partial^2 H'/\partial I_{sp}^2 < 0$ (convexity condition), 3) $I_{sp_{min}} \leq I_{sp} \leq I_{sp_{max}}$ (specific impulse constraint), and 4) $\tau = 1$ (thruster on). Consider the set $\mathcal{P}$ of pairs $(\bar{f}, \bar{I}_{sp})$ that satisfy the condition $\partial H'/\partial I_{sp} = 0$. Note that the set $\mathcal{P}$ is constituted by the solutions of Eq. (21). Clearly, $\bar{I}_{sp}$ maximizes H' provided $(\bar{f}, \bar{I}_{sp}) \in \mathcal{S}$. Under the assumption $c_2 \neq 0$, when $n = 2$ is substituted into Eq. (21) it is found that the set $\mathcal{P}$ coincides with the solutions of

$$I_{sp}^3 + [(c_1/c_2)f - c_0/c_2]I_{sp} + 2(c_0/c_2)f = 0 \tag{22}$$

However, the intersection of $\mathcal{P}$ with $\mathcal{S}$ may be empty or not, depending on the specific thruster data. The two situations are shown in Fig. 3 for the NSTAR thruster and in Fig. 4 for the NEXT thruster.

Consider first the NSTAR thruster. Because $\mathcal{P} \cap \mathcal{S} = 0$, the specific impulse maximizing H' is obtained for an extremal value of

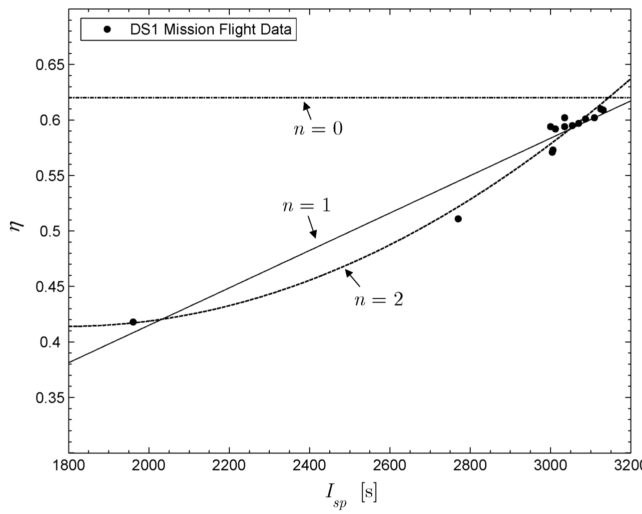

Fig. 1 Polynomial approximation of η vs I_{sp} for NSTAR thruster (derived from Ref. 20).

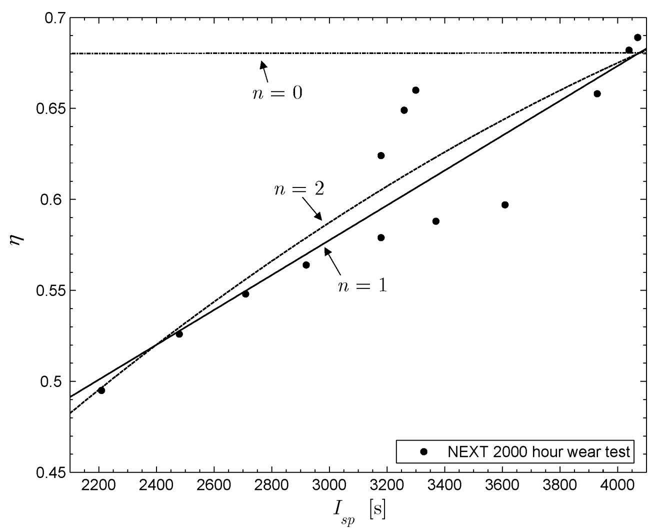

Fig. 2 Polynomial approximation of η vs I_{sp} for NEXT thruster (derived from Ref. 21).

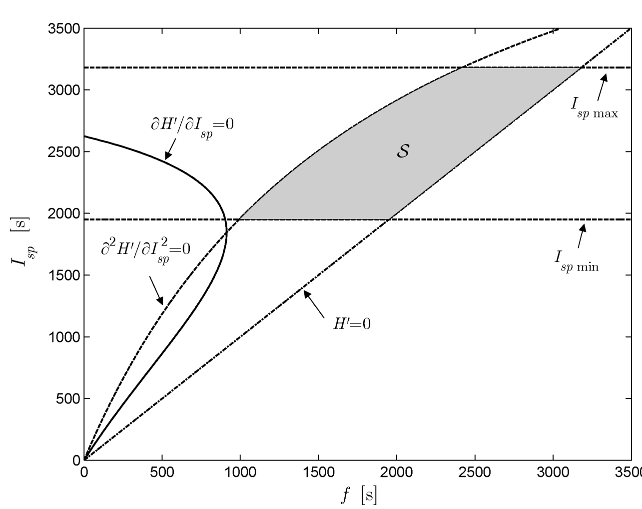

Fig. 3 Admissible region $\mathcal{S}$ with a quadratic approximation of η vs I_{sp} for NSTAR thruster.

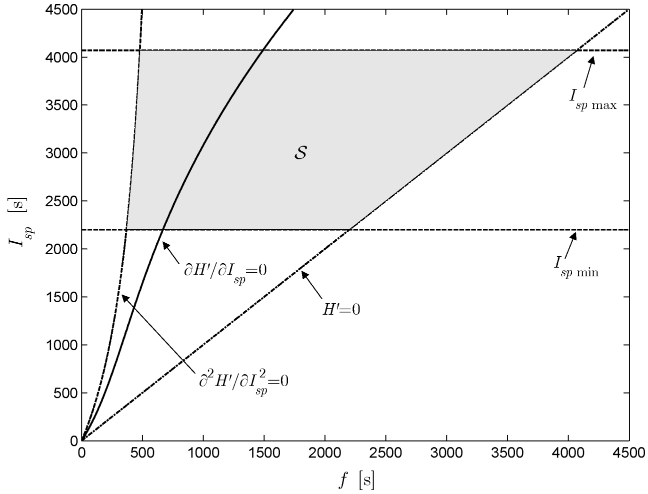

Fig. 4 Admissible region $\mathcal{S}$ with a quadratic approximation of η vs I_{sp} for NEXT thruster.

I_{sp} in the range (5). It is easily checked that $H'(I_{sp_{min}}) > H'(I_{sp_{max}})$ as long as $f < f^*$ and $H'(I_{sp_{min}}) < H'(I_{sp_{max}})$ whenever $f > f^*$, where f^* is that value of f that is obtained enforcing $H'(I_{sp_{min}}) = H'(I_{sp_{max}})$. The result is

$$f^* = \frac{I_{sp_{min}} I_{sp_{max}} \left(c_0 - c_2 I_{sp_{min}} I_{sp_{max}}\right)}{c_0 \left(I_{sp_{min}} + I_{sp_{max}}\right) + c_1 I_{sp_{min}} I_{sp_{max}}} \tag{23}$$

Accordingly, the optimal specific impulse control law for the NSTAR thruster is given by $I_{sp} = I_{sp}^*$, where

$$I_{sp}^* = \begin{cases} I_{sp_{min}}, & \text{if} \quad f < f^* \\ I_{sp_{max}}, & \text{if} \quad f > f^* \end{cases} \tag{24}$$

The NEXT thruster has a different behavior. From Fig. 4, it is clear that in this case the intersection of $\mathcal{P}$ with $\mathcal{S}$ is nonempty. Let f_{min} be the solution of Eq. (22) that corresponds to $I_{sp} = I_{sp_{min}}$ and f_{max} be the solution corresponding to $I_{sp} = I_{sp_{max}}$. Then, the optimal control law is in the form

$$I_{sp}^* = \begin{cases} I_{sp_{min}}, & \text{if} \quad f < f_{min} \\ \bar{I}_{sp}, & \text{if} \quad f_{min} \le f \le f_{max} \\ I_{sp_{max}}, & \text{if} \quad f > f^{max} \end{cases} \tag{25}$$

where $\bar{I}_{sp}$ is the specific impulse solution of Eq. (22).

Linear and Constant Approximation of η

In the case of a linear relationship between η and I_{sp} or a constant efficiency, it can be verified that the optimal control law is in the form of Eq. (25), where $\bar{I}_{sp}$ is the specific impulse obtained substituting $n = 1$ and $n = 0$ into Eq. (21). The result is

$$\bar{I}_{sp} = \begin{cases} \dfrac{2c_0 f}{c_0 - c_1 f}, & \text{if} \quad n = 1 \\ 2f, & \text{if} \quad n = 0 \end{cases} \tag{26}$$

Also, f_{min} and f_{max}, to be used in Eq. (25), are the values of f in Eq. (21) that correspond to $I_{sp} = I_{sp_{min}}$ and $I_{sp} = I_{sp_{max}}$, respectively. Note that the control law for $n = 0$, that is, $\eta = \text{const}$, agrees with the result by Kechichian[12] and Nah et al.[15]

The optimal control laws for the two thrusters and the three cases $n = 0$, 1, and 2 are shown in Figs. 5 and 6 as a function of f.

Numerical Examples

The boundary-value problem associated to the variational problem is constituted by the equations of motion (1–3) and the Euler–Lagrange equations (11–13). The boundary conditions are constrained by the planetary ephemerides based on the Jet Propulsion Laboratory DE405/LE405 model. They provide 12 scalar conditions connected to the position and velocity of the spacecraft at both $t = t_0$ and $t = t_f$. The other two boundary conditions are given by the spacecraft initial mass $m_0 = m(t_0)$ and the transversality condition $\lambda_m(t_f) = 1$.

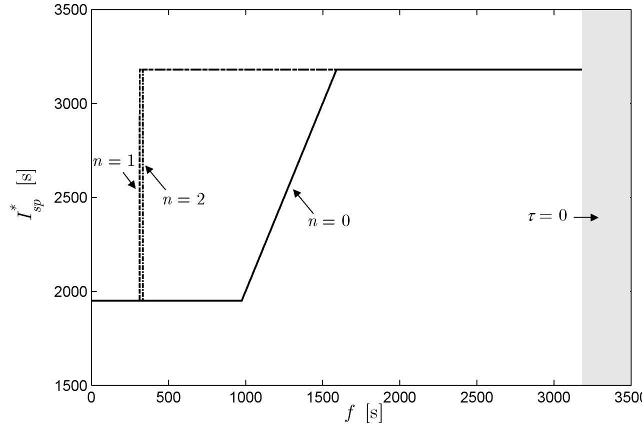

Fig. 5 Optimal specific impulse vs f for NSTAR thruster with $n = 0$, 1, and 2.

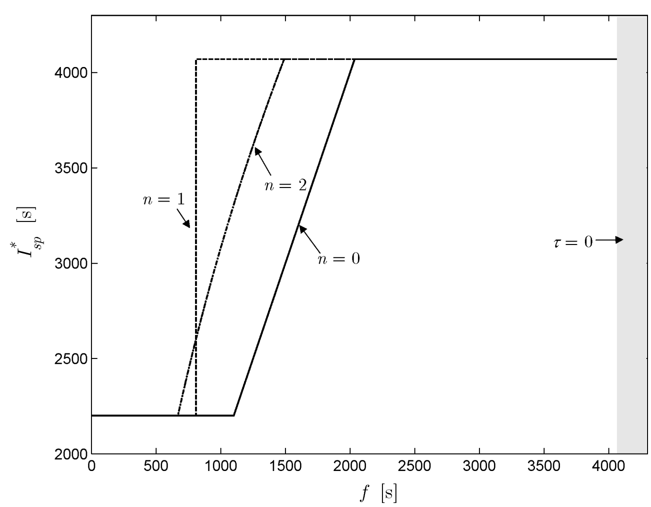

Fig. 6 Optimal specific impulse vs f for NEXT thruster with $n = 0$, 1, and 2.

A set of canonical units[22] have been used in the integration of the differential equations to reduce their numerical sensitivity. The differential equations were integrated in double precision using a Runge–Kutta fifth-order scheme with absolute and relative errors of 10^{-10}. The final boundary constraints were set to 1×10^5 km for the position error and to 0.7 km/s for the velocity error. These values are compatible with a preliminary mission design[23] and allow one to obtain mission data in a reasonable computational time.

Two Mars missions with NEXT and NSTAR thrusters are investigated. In both cases the coefficients $d_1, \ldots, d_5$ of Eq. (7), which establish the performance of the solar array, are taken from Williams and Coverstone-Carroll.[4] In particular, $d_1 = 1.1063$, $d_2 = 0.1495$, $d_3 = -0.299$, $d_4 = -0.0432$, and $d_5 = 0$. Orbiter missions with a Delta 2 class launch vehicle (1300-kg injected mass with a launch energy $C_3 = 0$) are assumed. Also, the power allocated to operate the spacecraft systems is $P_L = 400$ W (Ref. 5).

Mars Mission with NSTAR Thruster

The specific impulse of the NSTAR thruster is constrained to vary between $I_{sp_{min}} = 1950$ s and $I_{sp_{max}} = 3180$ s (Ref. 20), the maximum input power to the PPU is $P_P^{max} = 2.53$ kW, the solar array power at 1 astronomical unit (AU) is $P_\odot = 5$ kW and the duty cycle is $\eta_P = 0.9$.

Mars missions with NSTAR thrusters have been investigated by Williams and Coverstone-Carroll.[5] They have shown that when long

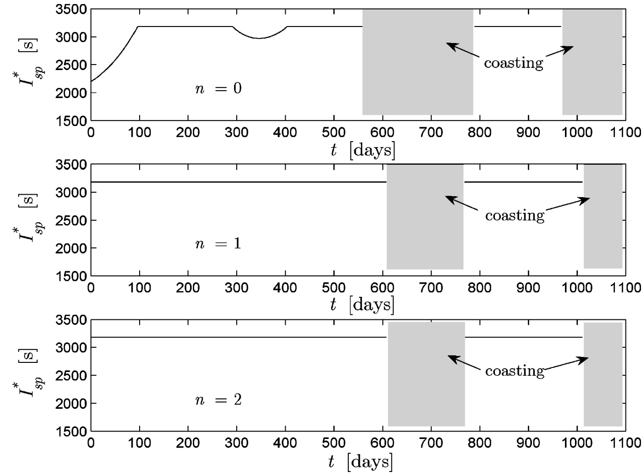

Fig. 7 Time history of the specific impulse for a Mars mission with NSTAR thruster (departure date 1 August 2006).

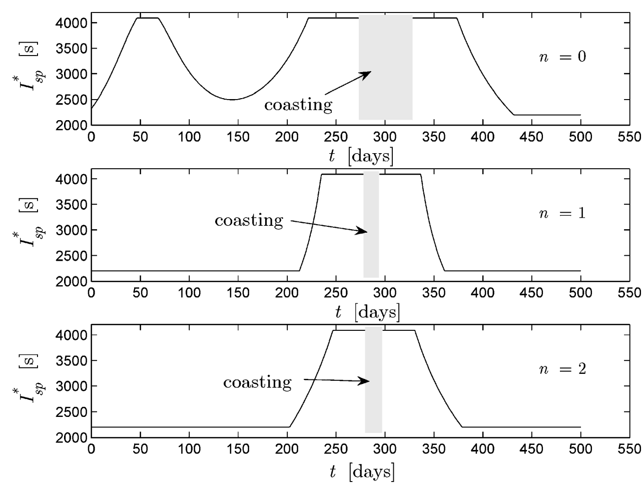

Fig. 8 Time history of the specific impulse for a fast Mars mission with NEXT thruster (departure date 1 April 2009).

flight times are considered, rather wide launch opportunities exist with near equivalent performance. When a time of flight of three years is assumed, fuel optimal launch dates are in the range June–December 2006 (Ref. 5). Accordingly, for comparative purposes we used 1 August 2006 as a departure date.

The optimal control laws for the specific impulse (Fig. 7), have two burn phases and two coast arcs for all of the three values of n; however, a modulated specific impulse is present only for $n = 0$. Note that there is coasting phase at the end of each trajectory. This amounts to an early rendezvous that is compatible with the final velocity tolerance. As far as the fuel consumption Δm is concerned, the results are $\Delta m = 199$ kg for $n = 0$ and $\Delta m = 213$ kg for $n = 1$ and $n = 2$. In all cases, Mars trajectories arrive with zero hyperbolic excess velocity. As a result, when an accurate model for the thruster efficiency is employed ($n = 2$), an increase of fuel consumption on the order of 7% is obtained with respect to the case of constant efficiency ($n = 0$).

Mars Mission with NEXT Thruster

The specific impulse of the NEXT thruster is constrained to vary between $I_{\mathrm{sp}_{\min}} = 2200$ s and $I_{\mathrm{sp}_{\max}} = 4090$ s (Ref. 21), the maximum input power to the PPU is $P_P^{\max} = 6.5$ kW, the solar array power at 1 AU is $P_\odot = 10$ kW, and the duty cycle is $\eta_P = 0.94$.

In this case, a fast mission with time of flight of 500 days and a departure date on 1 April 2009 has been investigated. Note that no attempt has been made to optimize the launch opportunity. The time histories of the optimal control laws for the specific impulse are shown in Fig. 8. In all three cases, phases with minimum, maximum, and intermediate values of I_{sp} are present. Also note that in all three cases a single coast arc exists in the trajectory. When a zero value of hyperbolic excess velocity at arrival is assumed, the results are $\Delta m = 321$ kg for $n = 0$, $\Delta m = 397$ kg for $n = 1$, and $\Delta m = 404$ kg for $n = 2$. Note that a quadratic variation of the thruster efficiency with the specific impulse corresponds to an increase of 25% of the fuel consumption with respect to the case of constant efficiency.

Conclusions

Fuel-optimal, time-fixed, three-dimensional trajectories for SEP-based missions have been discussed. Key features of the paper are the accommodation of the constraints on the specific impulse and a realistic model for the thruster efficiency. The latter is related to the instantaneous value of the specific impulse through a polynomial expression. The formulation takes into account the possibility of switching off the thruster and allowing coast arcs. The optimal control problem is solved using an indirect method. Experimental data for two different ion thrusters have been used to simulate realistic missions. The optimal specific impulse control law is shown to depend on the instantaneous values of the primer vector, the spacecraft mass, and the mass costate. It is observed that the structure of the specific impulse optimal control laws is different for the two thrusters.

Long-term and rapid interplanetary trajectories toward Mars have been investigated using two different ion thruster models. It has been shown that the choice of the degree of approximation of the thruster efficiency model significantly affects both the control law and the fuel consumption with respect to a constant efficiency model.

Acknowledgments

The authors acknowledge the anonymous reviewers for their valuable comments, which helped improve the presentation of this paper.

References

[1]Rayman, M. D., Varghese, P., Lehman, D. H., and Livesay, L. L., "Results from the Deep Space 1 Technology Validation Mission," *Acta Astronautica*, Vol. 47, No. 2–9, 2000, pp. 475–487.

[2]Brophy, J. R., and Noca, M., "Electric Propulsion for Solar System Exploration," *Journal of Propulsion and Power*, Vol. 14, No. 5, 1998, pp. 700–707.

[3]Brophy, J. R., "Advanced Ion Propulsion Systems for Affordable Deep-Space Missions," *Acta Astronautica*, Vol. 52, No. 2–6, 2003, pp. 309–316.

[4]Williams, S. N., and Coverstone-Carroll, V., "Benefits of Solar Electric Propulsion for the Next Generation of Planetary Exploration Missions," *Journal of the Astronautical Sciences*, Vol. 45, No. 2, 1997, pp. 143–159.

[5]Williams, S. N., and Coverstone-Carroll, V., "Mars Missions Using Solar Electric Propulsion," *Journal of Spacecraft and Rockets*, Vol. 37, No. 1, 2000, pp. 71–77.

[6]Kluever, C. A., "Comet Rendezvous Mission Design Using Solar Electric Propulsion Spacecraft," *Journal of Spacecraft and Rockets*, Vol. 37, No. 5, 2000, pp. 698–700.

[7]Sauer, C. G., Jr., "Solar Electric Performance for Medlite and Delta Class Planetary Missions," AAS/AIAA Astrodynamics Specialist Conf., American Astronautical Society, AAS Paper 97-726, Aug. 1997.

[8]Scheel, W., and Conway, B. A., "Optimization of Very-Low-Thrust, Many-Revolution Spacecraft Trajectories," *Journal of Guidance, Control, and Dynamics*, Vol. 17, No. 6, 1994, pp. 1185–1192.

[9]Tang, S., and Conway, B. A., "Optimization of Low-Thrust Interplanetary Trajectories Using Collocation and Nonlinear Programming," *Journal of Guidance, Control, and Dynamics*, Vol. 18, No. 3, 1995, pp. 599–604.

[10]Hartmann, J. W., Coverstone-Carroll, V., and Williams, S. N., "Optimal Interplanetary Spacecraft Trajectories via a Pareto Genetic Algorithm," *Journal of the Astronautical Sciences*, Vol. 46, No. 3, 1998, pp. 267–282.

[11]Kluever, C. A., "Optimal Low-Thrust Interplanetary Trajectories by Direct Method Techniques," *Journal of the Astronautical Sciences*, Vol. 45, No. 3, 1997, pp. 247–262.

[12]Kechichian, J. A., "Optimal Low-Thrust Transfer Using Variable Bounded Thrust," *Acta Astronautica*, Vol. 36, No. 7, 1995, pp. 357–365.

[13]Carter, T. E., and Pardis, C. J., "Optimal Power-Limited Rendezvous with Upper and Lower Bounds on Thrust," *Journal of Guidance, Control, and Dynamics*, Vol. 19, No. 5, 1996, pp. 1124–1133.

[14]Vadali, S. R., Nah, R. S., Braden, E., and Johnson, I. L., Jr., "Fuel-Optimal Planar Earth–Mars Trajectories Using Low-Thrust Exhaust-Modulated Propulsion," *Journal of Guidance, Control, and Dynamics*, Vol. 23, No. 3, 2000, pp. 476–482.

[15]Nah, R. S., Vadali, S. R., and Braden, E., "Fuel-Optimal, Low-Thrust, Three-Dimensional Earth–Mars Trajectories," *Journal of Guidance, Control, and Dynamics*, Vol. 24, No. 6, 2001, pp. 1100–1107.

[16]Auweter-Kurtz, M., and Kurtz, H., "Optimization of Electric Thrusters for Primary Propulsion Based on the Rocket Equation," *Journal of Propulsion and Power*, Vol. 19, No. 3, 2003, pp. 413–423.

[17]Sauer, C. G., Jr., "Modeling of Thruster and Solar Array Characteristics in the JPL Low-Thrust Trajectory Analysis," AIAA Paper 78-645, April 1978.

[18]Lawden, D. F., *Optimal Trajectories for Space Navigation*, Butterworths, London, 1963, pp. 54–68.

[19]Lewis, F. L., and Syrmos, V. L., *Optimal Control*, 2nd ed., Wiley, New York, 1995, pp. 284–290.

[20]Brophy, J. R., Kakuda, R. Y., Polk, J. E., Anderson, J. R., Marcucci, M. G., Brinza, D., Henry, M. D., Fujii, K. K., Mantha, K. R., Stocky, J. F., Sovey, J., Patterson, M., Rawlin, V., Hamley, J., Bond, T., Christensen, J., Cardwell, H., Benson, G., Gallagher, J., and Matranga, M., "Ion Propulsion System (NSTAR) DS1 Technology Validation Report," Jet Propulsion Lab., Technical Rept. JPL 00-10, Pasadena, CA, Oct. 2000.

[21]Soulas, G. C., Domonkos, M. T., and Patterson, M., "Wear Test Results for the NEXT Ion Engine," AIAA Paper 2003-4863, July 2003.

[22]Seidelmann, P. K., *Explanatory Supplement to the Astronomical Almanac*, Univ. Science Books, Mill Valley, CA, 1992, pp. 696, 697.

[23]Dachwald, B., "Minimum Transfer Times for Nonperfectly Reflecting Solar Sailcraft," *Journal of Spacecraft and Rockets*, Vol. 41, No. 4, 2004, pp. 693–695.